

Greening in the circumpolar high-latitude may amplify warming in the growing season

Jee-Hoon Jeong · Jong-Seong Kug · Baek-Min Kim ·
Seung-Ki Min · Hans W. Linderholm · Chang-Hoi Ho ·
David Rayner · Deliang Chen · Sang-Yoon Jun

Received: 1 November 2010 / Accepted: 6 July 2011 / Published online: 26 July 2011
© Springer-Verlag 2011

Abstract We present a study that suggests greening in the circumpolar high-latitude regions amplifies surface warming in the growing season (May–September) under enhanced greenhouse conditions. The investigation used a series of climate simulations with the Community Atmospheric Model version 3—which incorporates a coupled, dynamic global vegetation model—with and without vegetation feedback, under both present and doubled CO₂ concentrations. Results indicate that climate warming and associated changes promote circumpolar greening with northward expansion and enhanced greenness of both the Arctic tundra and boreal forest regions. This leads to additional surface warming in the high-latitudes in the growing season, primarily through more absorption of incoming solar radiation. The resulting surface and tropospheric warming in the high-latitude and Arctic regions weakens prevailing tropospheric westerlies over 45–70N,

leading to the formation of anticyclonic pressure anomalies in the Arctic regions. These pressure anomalies resemble the anomalous circulation pattern during the negative phase of winter Arctic Oscillation. It is suggested that these circulation anomalies reinforce the high-latitude and Arctic warming in the growing season.

Keywords Vegetation · Arctic warming · Arctic greening · Climate model · Future climate · Atmospheric circulation · Surface energy budget

1 Introduction

The high-latitude and Arctic regions have experienced substantial climate warming in recent decades. The degree and rate of warming in these regions has been much greater and faster than for the global average temperature due to various climate feedbacks (e.g. Rothrock et al. 1999; Serreze et al. 2000; ACIA 2005; Chapin et al. 2005; Screen and Simmonds 2010). Great attention has been paid to the changes in the vegetation-ecosystems in the high-latitude and Arctic regions during this climate warming and to their potential to generate feedbacks and cause further climate change (e.g. Chapin et al. 2005; Foley 2005).

Associated with recent increase in temperature and the extension of growing season, significant enhancement of vegetation greenness in the Arctic tundra and grassland areas has been observed (Tucker et al. 2001; Zhou et al. 2001; Bunn et al. 2007), and also the expansion of shrubs in Northern Alaska and pan Arctic regions (Tape et al. 2006). The physiological effect of rising CO₂ on vegetation (i.e., the CO₂ fertilization effect) is suggested to have also contributed to these changes by increased

J.-H. Jeong · H. W. Linderholm · D. Rayner · D. Chen
Department of Earth Sciences, University of Gothenburg,
Gothenburg, Sweden

J.-S. Kug (✉)
Korea Ocean Research and Development Institute, Ansan, Korea
e-mail: jskug@kordi.re.kr

B.-M. Kim
Korea Polar Research Institute, Incheon, Korea

S.-K. Min
Climate Research Division, Environment Canada, Toronto,
Canada

C.-H. Ho · S.-Y. Jun
School of Earth and Environmental Sciences,
Seoul National University, Seoul, Korea

photosynthesis of plants, particularly among C3 plants (Mooney et al. 1999). Such vegetation changes, in turn, affect the local climate system by altering the surface energy budget and hydrological cycle. For instance, if snow-covered or barren surfaces are replaced by vegetated surface, increased absorption of solar energy due to reduced surface albedo induces additional surface warming (Bonan et al. 1992; Foley et al. 1994; Chapin et al. 2005). On the other hand, an increase in vegetation activity has a surface-cooling effect if the enhanced vegetation activity induces a large increase in evapotranspiration from vegetated land surfaces (Jeong et al. 2009). Another possibility suggested is that an increase in vegetation activity (i.e., enhanced plant growth) may slow down the increasing concentration of CO₂ and alleviate warming by carbon sequestration, the uptake of the atmospheric CO₂ (Watson 2000). Hence it is widely recognized that the vegetation-climate feedback has a great potential to amplify or dampen either natural or anthropogenic climate change.

The significance of the vegetation-feedback effect for climate models' responses to anthropogenic climate forcings—and even to the paleo-climate perturbations—has been previously recognized (Bonan et al. 1992; Foley et al. 1994). Although the vegetation feedback operates differently depending on regional climate characteristics and vegetation types (Levis et al. 1999), climate model simulations generally suggest that the vegetation changes have a positive feedback effect on climate warming, particularly in the high-latitudes and Arctic—more vegetation growth feeds warming, which is mainly caused by reduced surface albedo (Bonan et al. 1992; Foley et al. 1994; Levis et al. 1999; Zhang and Walsh 2006; Notaro et al. 2007; Notaro and Liu 2008; O'ishi and Abe-Ouchi 2009; Swann et al. 2010).

The objective of the present study is to further investigate the role of vegetation feedback effects on the climate change response to greenhouse warming. By utilizing a fully coupled climate–vegetation model, a series of idealized simulations with present and doubled CO₂ concentration are performed, both with and without vegetation feedback. The contribution of vegetation feedbacks to the changes is quantitatively estimated from several sensitivity experiments. The vegetation feedback effect to surface air temperature (SAT) and the associated surface energy budget are analyzed, and the associated large scale circulation change and its role in driving climate change in the high-latitude and Arctic are discussed.

The modeling system used and experiments performed are described in Sect. 2, the estimated vegetation feedback effect and circulation change are presented in Sect. 3, followed by discussion and summary in Sect. 4.

2 Model experiments

2.1 Model description

To investigate the vegetation feedback effect under climate warming, a series of global climate model experiments are conducted using the Community Atmospheric Model version 3 (CAM3; Collins et al. 2004) an atmospheric general circulation model developed by the National Center for Atmospheric Research (NCAR). We use a version with a horizontal resolution of T42 (approximately 2.8° × 2.8°) and 26 hybrid-sigma vertical levels.

The land surface model incorporated with CAM3 is the Community Land Model version 3 (CLM3; Oleson et al. 2004), which adopts a dynamic global vegetation model (DGVM), a modified version of the Lund-Potsdam-Jena vegetation model (Sitch et al. 2003; Levis et al. 2004; and many references therein). The DGVM simulates the evolution of vegetation cover and structure under given climatic conditions. The DGVM represents global vegetation with 10 plant functional types (PFTs; see Table 2), and calculates every PFTs' leaf area index (LAI), canopy height, and fractional cover relative to the portion of the grid cell allocated to natural vegetation, which represents only 'non-agricultural' vegetation. Synchronous climate-vegetation coupling enables CAM3-DGVM to consider the biogeophysical and biogeochemical interactions between climate and vegetation. The plant-atmosphere exchange of CO₂ is parameterized by the DGVM, but the atmospheric concentration of CO₂ is set to be fixed in the current CAM3-DGVM because the terrestrial carbon cycles are not fully resolved. If not coupled to the DGVM, CAM3 runs with prescribed fractional cover and seasonal cycle of LAI of PFTs estimated from satellite observation.

2.2 Experimental design

A potential distribution of present-day vegetation is obtained by a spin-up simulation of the CAM3-DGVM for 500 years under 'present' climate forcings: i.e., 355 ppmv CO₂ concentration and observed climatological seasonal cycles (1961–1990) of sea surface temperatures (SST) and sea ice concentration derived from UK Met office Hadley center (Rayner et al. 2003). Evolving from an initial non-vegetated state, the simulated global vegetation fields reaches a quasi-equilibrium state in terms of the fractional cover and LAI of global vegetation from about model year 350. The 'present' vegetation field, a possible state of global vegetation which could be reached under the 'present' climate condition without the interference of human activity, is taken from an average of last 50 years of the 'spin-up' simulation'. The simulated 'present' vegetation field captures fairly-well the major vegetated area with

a reasonable seasonal cycle of plants' growth, despite some deficiencies (Levis et al. 2004).

Three ensemble experiments are performed to estimate the 'CO₂ radiative effect' and 'vegetation feedback effect' from climate change under doubled CO₂ concentration. A brief summary of the experiments are given in Table 1. The first experiment, referred to as P, is a 'P'resent climate simulation. The CO₂ concentration is fixed to 355 ppmv (observed concentration in year 1992), and concentrations for other GHGs are taken from observed values for the same year; for instance, CH₄ and N₂O concentrations are set to 1.7090 and 0.3080 ppmv, respectively. By turning off the DGVM, the 'present' vegetation field: the fractional coverage and seasonal cycles of LAI for each of PFTs from the spin-up simulation is prescribed for this P experiment. The second experiment, referred to F, is an idealized 'F'uture climate simulation. The CO₂ concentration is doubled to 710 ppmv, but the 'present' vegetation field is again prescribed. Consequently, the difference between the P and F simulation is attributed to the radiative forcing due to the doubled CO₂ concentration—'CO₂ radiative effect'. This term implicitly includes the contributions from changed sea ice and SST that arise under enhanced greenhouse conditions (see below). The third experiment, referred to FV, is another 'F'uture climate simulation with the doubled CO₂ concentration, but includes the 'V'egmentation feedback effect by turning on the DGVM. Accordingly, the vegetation is allowed to respond to the overlying climate conditions, and so provide a feedback effect to climate. Hence, the difference between the FV and F is considered as the 'vegetation feedback effect' associated with the climate warming that results from doubling CO₂ concentration.

In order to consider the ocean's impact on climate change, the climatological distribution of sea ice and SSTs derived from present and doubled CO₂ simulations of NCAR Community Climate System Model version 3 (CCSM3; Collins et al. 2006) are prescribed as boundary conditions for the present (P) and future (F and FV) experiments respectively. The main features of the SST and sea ice differences between the present and future simulations of CCSM3 are overall warming in the SST and reduced sea ice concentrations in the Arctic region and Antarctic (figure not shown). With respect to the present values, the sea ice concentration over the Arctic sea (north of 65N) shows a 33.70% decrease, and the global mean

SST increases by 1.62°C with relatively larger increase in the high-latitudes (1.89°C increase for 60N–90N) in the May to September average.

All three experiments (P, F, and FV) are integrated for 100 years, with 5 ensemble members initiated by taking slightly different atmospheric initial conditions. Considering the adjustment time for the model, only the results for last 50 years of the experiments are utilized for analysis. Here we mainly focus on the temperature and atmospheric circulation changes in the growing season (May–September). This is the primary growing season for most vegetation in the Northern Hemisphere, and hence when the vegetation feedback effect is expected to be most pronounced. Ensemble averages from three experiments are compared, where the CO₂ radiative and vegetation effect are defined as:

1. CO₂ radiative effect (F minus P)
2. Vegetation feedback effect (FV minus F)
3. All effect (FV minus P)

The statistical significance of each effect (i.e., a difference between two experiments) is calculated by a two-sided Student's *t* test based on the mean and standard deviation estimated from the 50-year simulation results.

3 Results

3.1 Vegetation change under doubled CO₂ concentration

CAM3 simulates surface temperature increases across the entire Northern Hemisphere (NH) in response to the elevated CO₂ concentration (Fig. 1). Most regions show SAT increases in the range of 1.5–2.5°C (2.1°C for NH average over land) where the degree of warming tends to be relatively larger over dry, high-latitude continental regions. The magnitude of warming is comparable to that shown by the IPCC AR4 models for the second half of twenty-first century under the A1B scenario; an increase of about 2–3°C over land surface during summer (c.f. Fig. 13 in Chapman and Walsh 2007). Due to the differences between the prescribed SST and sea ice climatologies in the present (P) and future (F and FV) experiments, the reduced Arctic sea ice concentration and warmer SSTs in the high-latitudes in the future experiments may contribute to the relatively large warming in the high-latitude coastal regions. Precipitation also increases for most parts of the NH, particularly in high-latitude regions (Fig. 1b). Over some mid-latitudes, e.g. the southern Europe and western North America, drier conditions are found. This feature results from atmospheric circulation changes associated with elevated CO₂ concentration (Solomon et al. 2007). In general,

Table 1 Summary of experiments performed

	Vegetation	CO ₂	SST/SIC
P	Present prescribed	Present	Present
F	Present prescribed	Future	Future
FV	DGVM	Future	Future

Fig. 1 **a** The growing season (MJJAS) SAT and **b** precipitation change by the all effect (FV-P). Areas with a difference significant at the 99% confidence level are stippled

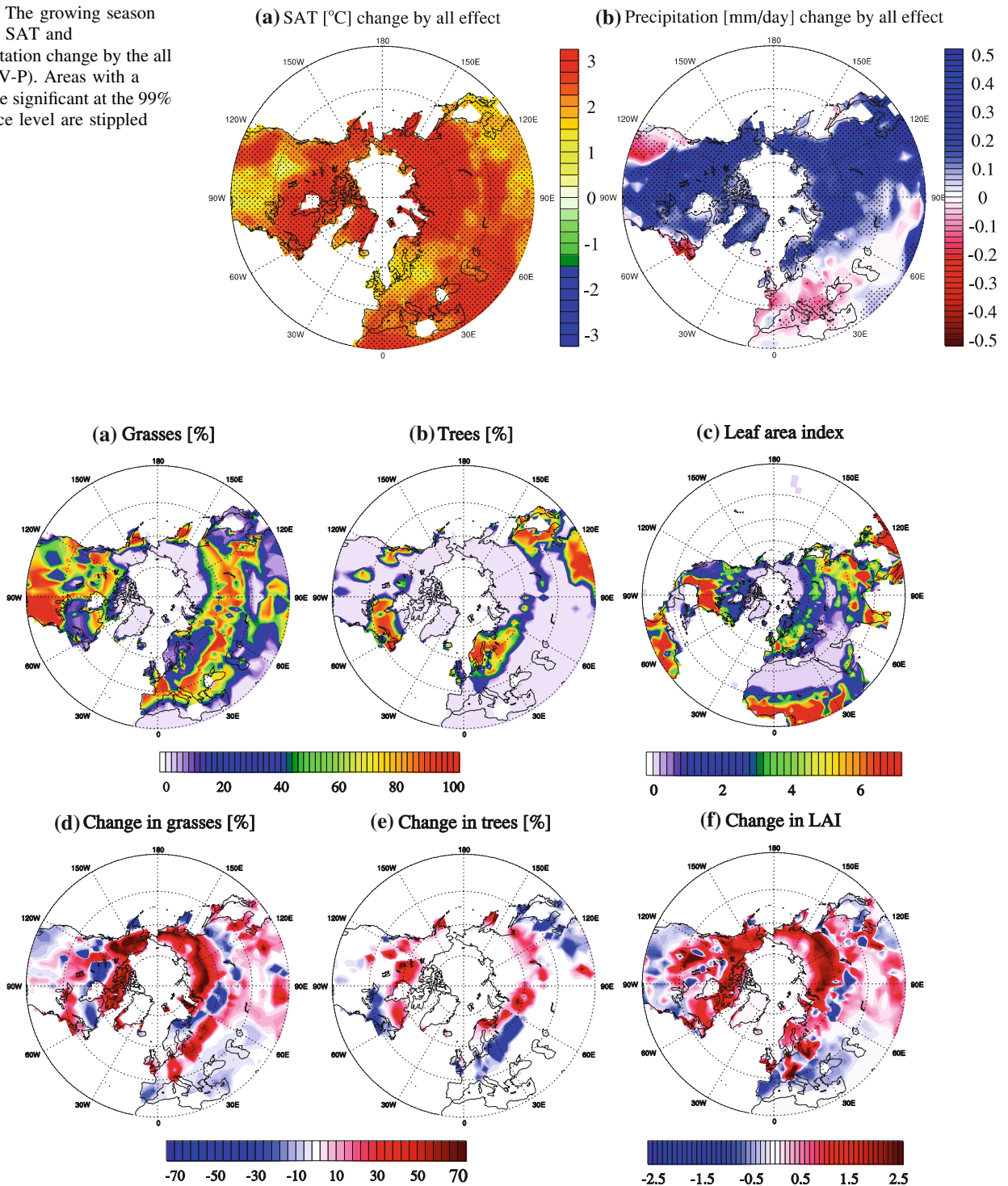


Fig. 2 Mean fractional cover of **a** grass and **b** tree species, and **c** mean leaf area index in the warm season under present level of CO₂ concentration (P). **d–f** their change due to doubled CO₂ (i.e. FV-P)

strong increases in temperature and precipitation in the Arctic and high-latitudes are most distinct, being consistent with results from previous observational and modeling studies (Chapman and Walsh 2007; Solomon et al. 2007; Min et al. 2008).

These changes in climate conditions affect the plant's establishments and growth, in addition to a direct physiological effect on plant's photosynthesis from the CO₂ fertilization effect. Therefore, global vegetation exhibits considerable changes in its fractional coverage and LAI

under a doubled CO₂ climate. Figure 2 and Table 2 represent the overall vegetation change in the NH corresponding to a doubled CO₂ climate. The most notable changes are found over the high-latitudes, north of 60N. The northward expansion and greening of plants are conspicuous over the northern rim of the high-latitude continents where low temperature and low radiation input are major environmental controls over plant's growth (Chapin 1983, 1987). The fractional covers of all PFTs increase, particularly for the Arctic grass group which more-than doubled (15.68–35.24%) its fractional coverage. Along with the increase in the fractional coverage of vegetation, the vegetation greenness greatly increases over the high-latitudes; LAI increase from 0.70 for the P simulation to 1.49 for the FV simulation. On the other hand, the vegetation changes in the mid-latitudes (30–60N) are relatively modest. The fractional coverages of C3 non-arctic grass and boreal broadleaf deciduous PFTs increase (29.62–34.60 and 4.94–5.52% respectively) but those of other plant species decrease slightly. The LAI slightly increases on average (2.42–2.61) but varies with location. A decrease in the LAI is detectable in western USA and

southwestern Europe, where the growing season precipitation decreases slightly (Fig. 1b).

3.2 Vegetation feedback effect on SAT

The most pronounced feature of vegetation feedback effect on SAT is warming over high-latitude land areas associated with circumpolar greening (Fig. 3a). Large increases in SAT are found in the northernmost region of the Eurasian and North American continents. The average SAT anomaly resulting from the vegetation feedback effect for the land areas in north of 60N is 0.3°C. This warming effect is most pronounced in June and July; the area-averaged SAT change in the north of 60N is 0.59 and 0.47° respectively, and become insignificant in August and September (0.20 and –0.02°C in the north of 60N) when plant activity in the high-latitude start to cease. In contrast, cooling dominates the mid-latitude land areas over North America, Western Europe, and East Asia. The zonal mean SAT change clearly shows the meridional structure of the vegetation feedback effect (Fig. 3b): enhanced warming of up to 0.4°C in the high-latitude north of 50N, and slight cooling

Table 2 Fractional [%] cover of each PFT simulated by CAM3-DGVM under present (P) and doubled concentration of CO₂ (FV) and its change (FV-P)

Tree species	High-latitudes (60–90N)			Mid-latitudes (30–60N)		
	P	FV	FV-P	P	FV	FV-P
Temperate needleleaf evergreen	0.41	0.45	+0.03	1.20	0.89	–0.31
Boreal needleleaf evergreen	2.98	3.62	+0.64	6.69	6.40	–0.29
Temperate broadleaf evergreen	0.00	0.01	+0.01	0.94	0.80	–0.13
Temperate broadleaf deciduous	2.32	3.09	+0.77	6.49	6.19	–0.29
Boreal broadleaf deciduous	2.13	4.43	+2.30	4.94	5.52	+0.58
c3 arctic grass	15.68	35.24	+19.56	16.29	15.05	–1.24
c3 non-arctic grass	2.66	5.35	+2.69	29.62	34.60	4.97

Tropical broadleaf evergreen and temperate broadleaf evergreen, which are not found (zero fractional cover) over the domain for both P and FV, are not listed

Fig. 3 Vegetation feedback effect (FV-F) on **a** growing season SAT changes. Areas with a significant difference at the 99% confidence level are stippled. **b** zonal mean growing season SAT changes by all (FV-P; *black solid line*), CO₂ radiative (F–P; *red dashed line*), and vegetation feedback (FV-F; *blue dotted line*) effect in the growing season. The SAT is averaged over land

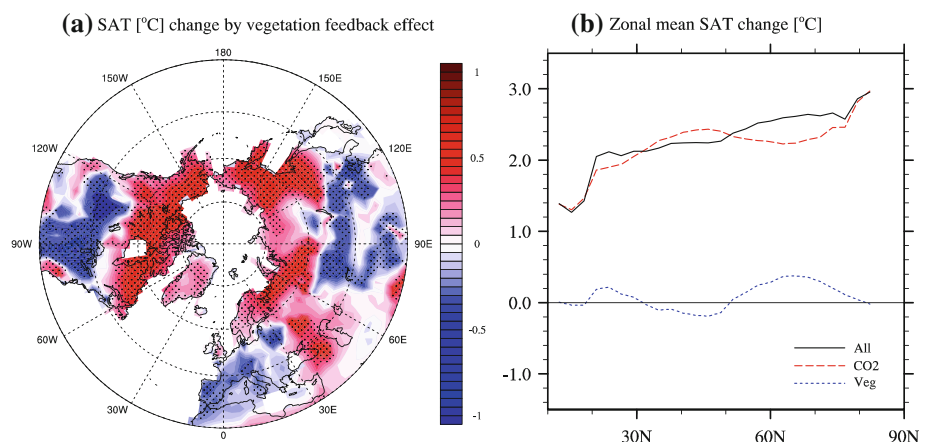
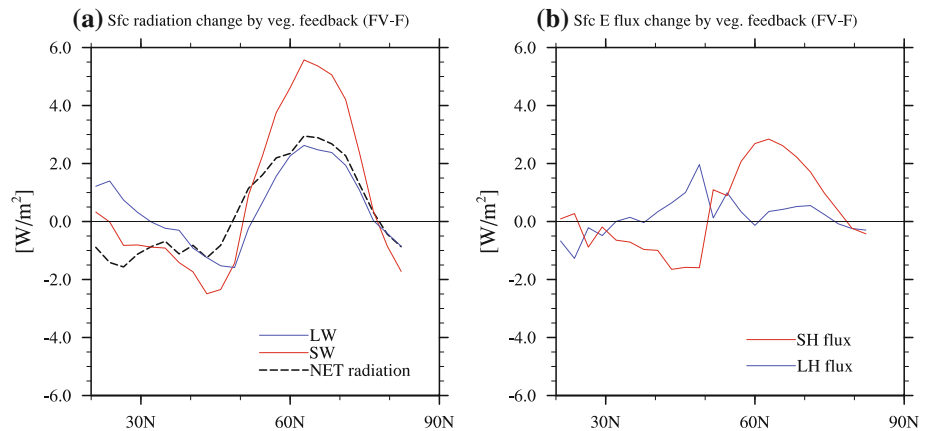


Fig. 4 Vegetation feedback effect (FV-F) on **a** zonal mean changes in absorbed SW (positive downward), emitted LW (positive upward), and net radiation (positive downward) at surface, and **b** zonal mean surface sensible and latent heat change (positive upward) over land in the growing season



in the mid-latitudes. The well-defined meridional structure and contrast in SAT changes between the high- and mid-latitudes provides the potential to induce atmospheric circulation change. This will be discussed further in the next section.

Two different physical feedback effects associated with the circumpolar greening can be considered as primary contributions to the SAT change; a decrease in surface albedo causes additional surface warming while an increase in latent heat (LH) fluxes associated with an increase in transpiration causes surface cooling. The change in surface radiation, and surface sensible heat (SH) and LH flux by vegetation change (Fig. 4) manifest the different contribution of the two feedback effects on the SAT change. In the high-latitude land regions (50–70N), an increase in absorbed shortwave radiation at surface ($\text{SW}\downarrow$) is notable. This is consistent with the vegetation increase in high-latitude regions, where increased vegetation cover and leaf abundance (i.e. higher LAI) reduces the surface albedo. Decreasing cloud cover over the high-latitude regions where the SAT warming is prominent additionally contributes to the increase in $\text{SW}\downarrow$, but the change is considered to be modest (figure not shown). The emitted longwave radiation ($\text{LW}\uparrow$) increases with increased surface temperature, but the magnitude is about the half of the $\text{SW}\downarrow$ increase (Fig. 4a). Consequently, there is a surplus in net incoming radiation at the surface, which is mostly balanced with an increase in sensible heat (SH) release from surface (Fig. 4b). On the other hand, latent heat (LH) only increases slightly associated with a modest increase in precipitation from the vegetation feedback effect (figure not shown), causing a modest (evaporative) cooling effect at surface. Therefore, these feedbacks cause a net warming effect on near-surface air temperature.

In the mid-latitudes (30–50N), both the $\text{SW}\downarrow$ and $\text{LW}\uparrow$ decrease from the vegetation feedback effect. As the decrease in $\text{SW}\downarrow$ is larger than the decrease in $\text{LW}\uparrow$, there is a net radiative cooling at the surface, which is mostly

balanced with a decrease in SH flux. The vegetation changes in the mid-latitudes are horizontally uneven when compared to the changes in the circumpolar high-latitudes. This implies that vegetation feedbacks may cause other effects that induce cooling in the mid-latitudes. The large-scale atmospheric circulation change by vegetation feedback, discussed in next section, contributes a cooling effect in the mid-latitudes, which partially offsets surface warming from increased CO_2 .

3.3 Circulation changes from the vegetation feedback effect

The circulation changes from the vegetation feedback effect are investigated by examining changes in atmospheric sea level pressure (SLP) and geopotential height (Z) (Fig. 5). There is an anomalous positive pressure center in Arctic region north of 50N, while negative pressure anomalies are found in the mid-latitudes over the north Pacific, East Asia, and northeastern America. Interestingly, this arctic high pressure/mid-latitude low pressure pattern in the growing season resembles the anomalous SLP pattern found during the negative phase of the AO, a primary internal dynamical mode of large-scale atmospheric circulation variability (Thompson and Wallace 1998). Despite less pronounced mid-latitude centers in the North Atlantic and North Pacific compared to those in the winter AO pattern, the hemispheric pattern of the anomalous SLP and Z at 500 and 200 hPa exhibit a well-defined negative AO-like structure. The structure extends from surface (Fig. 5a) through the mid- to upper-troposphere (Fig. 5b–c), and becomes more zonally-symmetric in the upper troposphere.

This negative AO-like circulation change is sustained by the circumpolar warming arising from the vegetation feedback effect. The vertical structures of the tropospheric wind and temperature changes from the vegetation feedback effect reveal a systematic dynamical relationship

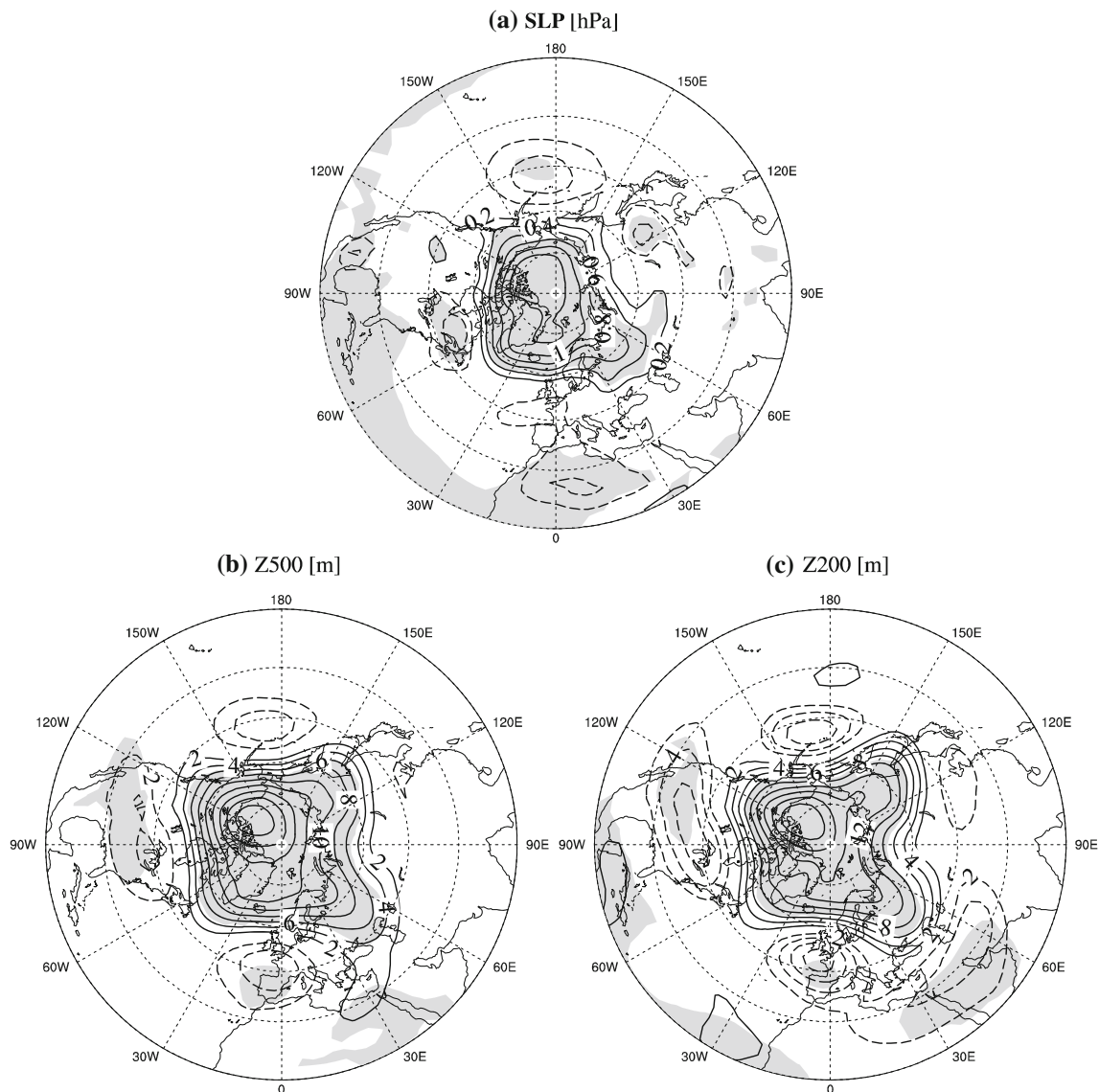


Fig. 5 Changes in **a** SLP, **b** Z at 500, and **c** 200 hPa in the growing season by the vegetation feedback effect (FV-F). *Solid and dashed lines indicate positive and negative values respectively, and gray shading indicates area with a significant difference at the 99% confidence level*

between the circumpolar warming and circulation change (Fig. 6a). Tropospheric warming from the vegetation feedback is distinct over 50–70N from the surface to lower to mid troposphere, extending to the Arctic region aloft. Surface warming in the Arctic region in winter tends to be mostly confined to near the surface due to very stably-stratified atmospheric conditions (Tjernström and Graveren 2009). However, the atmosphere is less stable in the growing season, so moderate vertical mixing enables the lower tropospheric warming to be transported to the mid and upper troposphere. Additionally, an increase in surface roughness by the enhanced vegetation can induce more turbulence and vertical mixing by lowering aerodynamic resistance (Bonan 2008). Along the southern flank of the circumpolar warming, negative westerly wind anomalies

throughout the troposphere are found around 50–70N, with a maximum at 60N at 300–250 hPa. The latitudes of maximum decrease in zonal wind almost coincide with the latitudes of maximum increase in SAT. To a large extent, the anomalous wind and tropospheric temperature changes from the vegetation feedback satisfy a thermal wind balance relationship. The easterly wind anomalies, extending to the upper troposphere with a maximum value at 300 hPa, coincide with the decreased meridional temperature gradient caused by the circumpolar warming. The maximum altitude of the easterly wind anomalies is dynamically linked with the existence of the significant cooling over the polar cap region above 300 hPa. Kug et al. (2010a, b) pointed out that such anomalous anticyclonic flow (i.e. a weakened polar vortex) induces a divergence of

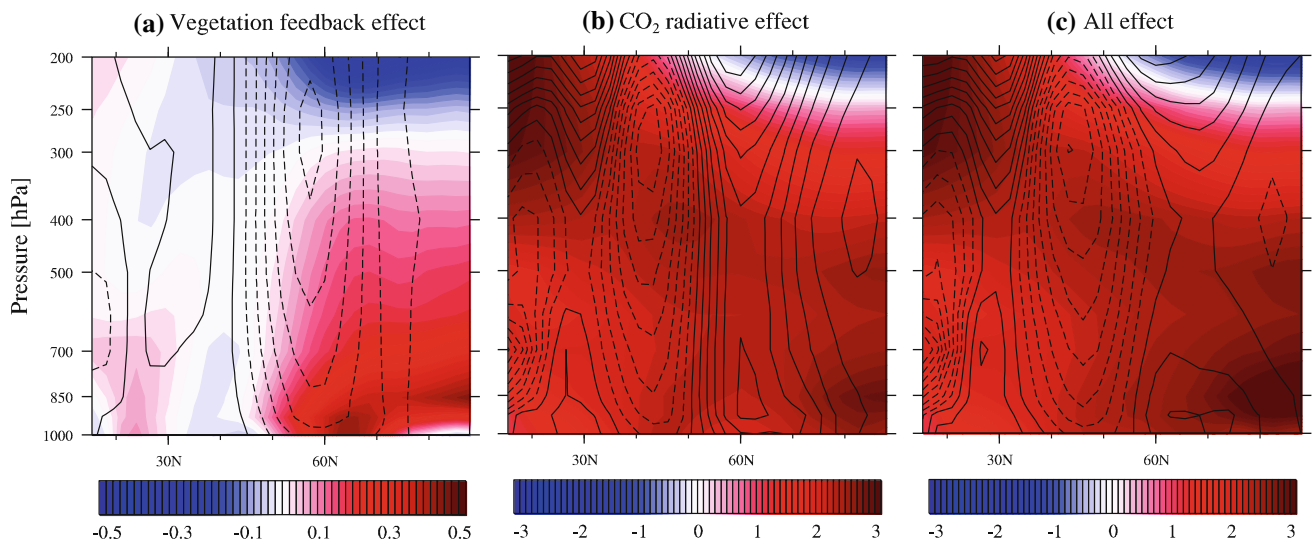


Fig. 6 Zonal mean temperature (*shading*, unit: K) and zonal wind (*contours*, unit: m s^{-1}) change in the growing season by **a** vegetation feedback effect (FV-V), **b** CO_2 radiative effect (F-P), and **c** all effects (FV-P). The contour interval of zonal wind is 0.01 m s^{-1}

heat flux by synoptic eddies, which leads to atmospheric cooling in the upper troposphere.

The atmospheric circulation changes caused by vegetation feedback (Fig. 6a) are clearly discernable even when compared with that induced by the CO_2 radiative effect (Fig. 6b), although the temperature change from vegetation feedback (Fig. 6a) is much smaller than that from the CO_2 effect (Fig. 6b). Perhaps this is because the changes in vegetation and associated surface temperature exhibit a zonally-elongated structure mostly concentrated around 50–70N, where the strong meridional temperature gradient with the strongest upper-level westerlies are found in summer. Hence such well-defined, large-scale anomalous temperature anomalies could efficiently induce large-scale circulation anomalies. Contrasting to the negative AO-like change from the vegetation feedback, the zonal wind changes from the CO_2 effect resemble the pattern of the positive AO phase; the zonal wind is strengthened over 50–70N while is slightly weakened in the mid-latitudes over 30–50N, indicating northward shift of the mid-latitude jet. Thus the circulation changes caused by vegetation feedback effect tend to counteract those caused by the CO_2 radiative effect. Interestingly, the anticyclonic circulation anomalies in the Arctic from the vegetation feedback effect also contrast with the cyclonic circulation anomalies over the Arctic found in climate model experiments forced by reduced sea ice in summer and autumn (Alexander et al. 2004; Deser et al. 2010).

This atmospheric circulation change is not just a response associated with the surface changes, but seemingly plays an additional role in reinforcing the vegetation feedback effect (Figs. 3, 4). The anticyclonic circulation anomalies in the Arctic and high-latitude regions may lead

to less cloudiness and more absorption of shortwave radiation at surface, which promote surface warming. The surface cooling in the mid-latitudes caused by the vegetation feedback can be partly explained by the cyclonic circulation anomalies. The anticyclonic anomaly and reduced zonal wind may allow more cold air from the Arctic to move southward, resulting in a cooling effect in the mid-latitudes, as suggested by Overland and Wang (2010). An increased cloudiness from the cyclonic circulation anomalies in the mid-latitudes may also provide a cooling effect.

4 Summary and discussion

In the present study, the possible amplification of high-latitude and Arctic warming in the growing season by vegetation feedbacks is investigated. Coupled vegetation-climate model simulations suggest that, in the growing season, circumpolar greening in the high-latitude amplifies surface warming, primarily by inducing more absorption of incoming SW radiation. In addition, our modeling results show that large-scale circulation changes arising from the vegetation feedback effects further strengthen the Arctic warming by forming high-pressure anomalies over the Arctic sea. In accordance with previous studies, the present results again emphasize the importance of incorporating vegetation feedback effects into climate change projections. Because the climate change projections of the IPCC AR4 were modelled with fixed (present day) vegetation, our results indicate that the IPCC projections may have underestimated the warming over the polar region, but overestimated the warming over the mid-latitudes.

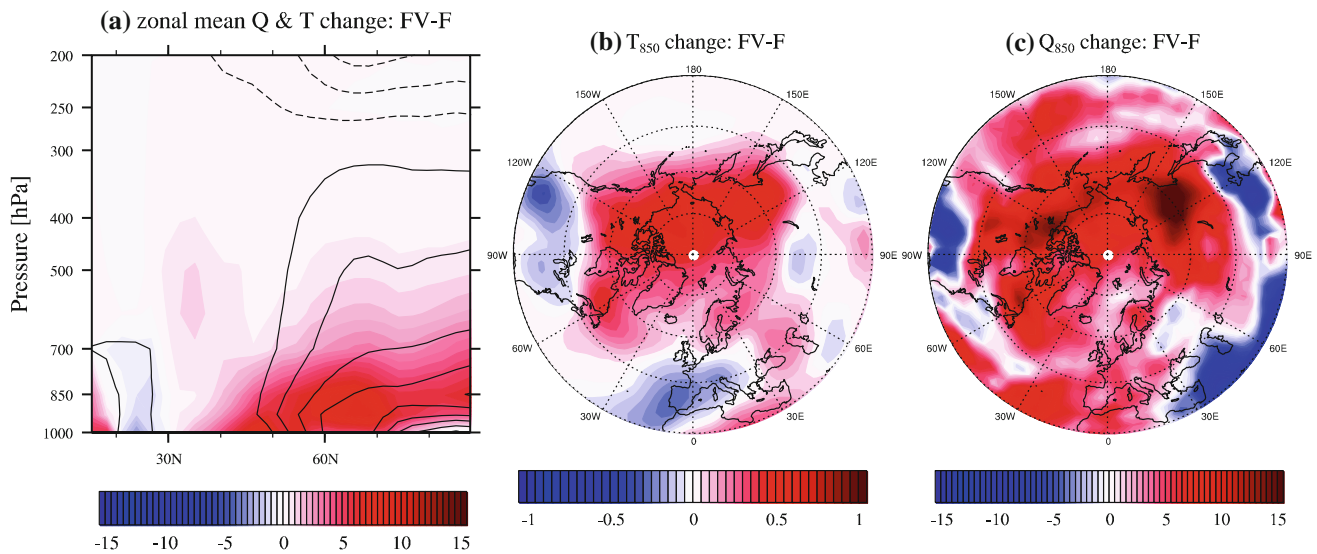


Fig. 7 a Zonal mean specific humidity (shading, unit: $\times 10^{-5}$ g/kg) and temperature (contours, unit: $^{\circ}\text{C}$) change by vegetation feedback effect (FV-F). The contour interval of temperature is 0.1°C . Changes

in b temperature and c specific humidity at 850 hPa in the growing season by vegetation feedback effect

In winter, the diminishing Arctic sea ice is the main driver of the amplified surface warming in the Arctic region under increasing concentrations of greenhouse gases (Screen and Simmonds 2010), and the arctic amplification is further contributed by the enhanced greenhouse effect associated with increases in water vapor (Schneider et al. 1999). Despite being less prominent in the growing season, the feedback associated with water vapor increases also contributes to the amplified warming in growing season through the vegetation feedback. In addition to the increased moisture-holding capability due to the warmer temperature, enhanced surface evapotranspiration by enhanced vegetation activity may induce an increase in tropospheric moisture content over the high-latitude and Arctic region (Fig. 7). It is very likely that the additional greenhouse effect caused by water–vapor feedback reinforces the Arctic warming in the lower to mid troposphere. Indeed, modeling by Swann et al. (2010) suggested that the Arctic warming induced by increased water–vapor from enhanced transpiration is up to 1.5 times larger than the warming induced by albedo changes from conversion of the bare ground to deciduous forests.

There are some important caveats when interpreting the results of this study. The suggested Arctic warming and circulation change caused by the vegetation feedback may lead to additional changes in sea ice and ocean circulation, but this is not taken into consideration in our present modeling system. Certainly, such changes could affect the ocean circulation and sea ice cover and thickness, which would invoke considerable feedback effects. For instance, the anticyclonic atmospheric circulation response from the vegetation feedback effect (Fig. 5) may cause sea ice

change. The Ekman drift associated with the anticyclonic circulation in the Arctic tend to move ice away from the coast, which consequently will reduce the overall ice area (Ogi and Wallace 2007). Such sea ice changes may then affect the climate in the following autumn and winter, as well as summer. Besides, the Arctic warming and humidity increases caused by the vegetation feedback effect are not confined to sub-Arctic landmasses, but span most parts of the Arctic Ocean (see Fig. 7b, c). Presumably this also enhances the Arctic warming by melting more sea ice. Swann et al. (2010) shows this feedback effect can be arisen by the vegetation feedback in the high-latitudes. We plan to address these issues with a series of experiments by using a GCM with fully sea ice and ocean model.

Also the limitations of the DGVM need to be carefully noted. First, the simulated potential vegetation has discrepancies against observed vegetation. CAM3-DGVM tends to underestimate the forest cover, but overestimate the grass cover (Bonan and Levis 2006). This is also the case in the simulated vegetation in northern high-latitudes. Another important discrepancy is the missing treatment of some important plant species in the Arctic ecosystem such as shrubs, sedges, and mosses. Especially, an increase in abundance and extent of shrubs in tundra area is one expected response to climate warming (Walker and Coauthors 2006). Compared to other arctic plants in the tundra, shrubs have a lower albedo and a stronger interaction with snow, and therefore a stronger positive feedback effect on the climate warming is expected (Sturm et al. 2001; Chapin et al. 2005). Grass and some other tree species undertake the shrub's role in the present CCSM3-DGVM and the simulated vegetation changes. However, in

a broad sense, the simulated change in vegetation under an elevated CO₂ concentration reflects the ‘more greening in the high-latitudes under surface warming’ that has been widely suggested by previous observation and modeling studies (e.g. Levis et al. 1999; Notaro et al. 2007; Swann et al. 2010). Therefore, the suggested feedback effects provide possible consequences from the enhanced vegetation in the high-latitudes, despite the discrepancies and limitations mentioned above. The second limitation with the usage of DGVM is that the vegetation feedback effect based on ‘potential’ vegetation change can be unrealistic in regions where there are large anthropogenic influences on land-use. Anthropogenic land-use changes, such as cultivation, irrigation, urbanization, and deforestation, have greatly influenced local climate, but this was not taken into account in the present modeling system. Necessarily, such considerations may have crucial influences on regional-scale climate changes, as well as on hydrological and biogeochemical changes. However, Myhre et al. (2005) estimated the radiative forcing caused by anthropogenic vegetation changes between pre-agricultural times to present to be modest in global average (-0.09 Wm^{-2}), and minimal in the high-latitudes where this study is focussed. Also to note is that changes in the carbon cycle by vegetation, and their possible feedback effects on climate change, are not considered in the present study. The atmospheric concentration of CO₂ is considerably modulated by vegetation’s uptake and storage of carbon, and the overlying climate determines the efficiencies of those processes. In particular, the present study suggests a large vegetation increase and amplified warming by the vegetation feedback effect over the permafrost regions where massive amount of organic carbon are stored in soils (Schoor et al. 2008). Because thawing permafrost, from warming and the resulting microbial decomposition of frozen organic carbon, is expected to give a significant feedback effect by releasing carbon to the atmosphere (Davidson and Janssens 2006; Zimov et al. 2006; Schoor et al. 2008), the competition between carbon uptake from above-ground greening and microbial decomposition of below-ground organic carbon needs to be carefully examined in order to accurately predict the climate feedbacks from terrestrial ecosystems under a changing climate.

Acknowledgments JH Jeong acknowledges support from the centre of Earth System Science at University of Gothenburg (TELLUS) and APEC Climate Center (APCC) international research project. BM Kim was supported by Korea Meteorological Administration Research and Development Program under Grant RACS_2011-2019 (PN11020). JS KUG was supported by KORDI (PE98651). This work was partly supported by the National Research Foundation of Korea (NRF) grant funded by the Korea government (MEST) (No. 20090093458). The authors are thankful for technical support for CAM3-DGVM experiments by Dr. Su-Jong Jeong, and the insightful comments from three anonymous reviewers.

References

- Alexander MA, Bhatt US, Walsh JE, Timlin MS, Miller JS, Scott JD (2004) The atmospheric response to realistic Arctic sea ice anomalies in an AGCM during winter. *J Climate* 17(5):890–905
- ACIA (2005) Arctic Climate Impact Assessment. Cambridge University Press, Cambridge
- Bonan GB (2008) Ecological climatology: concepts and applications. Cambridge University Press, Cambridge
- Bonan GB, Levis S (2006) Evaluating aspects of the community land and atmosphere models (CLM3 and CAM3) using a dynamic global vegetation model. *J Climate* 19(11):2290–2301
- Bonan GB, Pollard D, Thompson SL (1992) Effects of boreal forest vegetation on global climate. *Nature* 359(6397):716–718
- Bunn AG, Goetz SJ, Kimball JS, Zhang K (2007) Northern high-latitude ecosystems respond to climate change. *EOS* 88(34):333–340
- Chapin FS (1983) Direct and indirect effects of temperature on arctic plants. *Polar Biol* 2(1):47–52
- Chapin FS (1987) Environmental controls over growth of tundra plants. *Ecol Bull* 38:69–76
- Chapin FS, Sturm M, Serreze MC, McFadden JP, Key JR, Lloyd AH, McGuire AD, Rupp TS, Lynch AH, Schimel JP, Beringer J, Chapman WL, Epstein HE, Euskirchen ES, Hinzman LD, Jia G, Ping CL, Tape KD, Thompson CDC, Walker DA, Welker JM (2005) Role of land-surface changes in Arctic summer warming. *Science* 310(5748):657–660
- Chapman WL, Walsh JE (2007) Simulations of Arctic temperature and pressure by global coupled models. *J Climate* 20(4):609–632
- Collins WD, Rasch PJ, Boville BA, Hack JJ, Williamson DL, Kiehl JT, Briegleb B, Bitz C, Lin S-J, Zhang M, Dai Y (2004) Description of the NCAR community atmosphere model (CAM 3.0). National Center for Atmospheric Research, Boulder, Colorado
- Collins WD, Bitz CM, Blackmon ML, Bonan GB, Bretherton CS, Carton JA, Chang P, Doney SC, Hack JJ, Henderson TB, Kiehl JT, Large WG, McKenna DS, Santer BD, Smith RD (2006) The Community Climate System Model version 3 (CCSM3). *J Climate* 19(11):2122–2143
- Davidson EA, Janssens IA (2006) Temperature sensitivity of soil carbon decomposition and feedbacks to climate change. *Nature* 440:165–173
- Deser C, Tomas R, Alexander M, Lawrence D (2010) The seasonal atmospheric response to projected arctic sea ice loss in the late twenty-first century. *J Climate* 23(2):333–351
- Foley JA (2005) Tipping points in the tundra. *Science* 310(5748):627–628
- Foley JA, Kutzbach JE, Coe MT, Levis S (1994) Feedbacks between climate and boreal forests during the Holocene Epoch. *Nature* 371(6492):52–54
- Jeong SJ, Ho CH, Jeong JH (2009) Increase in vegetation greenness and decrease in springtime warming over east Asia. *Geophys Res Lett* 36:L02710
- Kug J-S, Choi D-H, Jin F-F, Kwon W-T, Ren H-L (2010a) Role of synoptic eddy feedback on polar climate responses to the anthropogenic forcing. *Geophys Res Lett* 37(14):L14704
- Kug J-S, Jin F-F, Park J, Ren H-L, Kang I-S (2010b) A general rule for synoptic-eddy feedback onto low-frequency flow. *Clim Dyn* 35(6):1011–1026
- Levis S, Foley JA, Pollard D (1999) Potential high-latitude vegetation feedbacks on CO₂-induced climate change. *Geophys Res Lett* 26(6):747–750
- Levis S, Bonan GB, Vertenstein M, Oleson KW (2004) The community land model’s dynamic global vegetation model (CLM-DGVM). National Center for Atmospheric Research, Boulder, Colorado

- Min SK, Zhang XB, Zwiers F (2008) Human-induced arctic moistening. *Science* 320(5875):518–520
- Mooney HA, Canadell J, Chapin FS, Ehleringer JR, Körner C, McMurtrie RE, Parton WJ, Pitelka LF, Shulze E-D (1999) Ecosystem physiology responses to global change. In: Walker BH, Steffen W, Canadell JG, Ingram J (eds) *Terrestrial biosphere and global change: implications for natural and managed ecosystems*. Cambridge University Press, Cambridge, pp 141–149
- Myhre G, Kvalevåg MM, Schaaf CB (2005) Radiative forcing due to anthropogenic vegetation change based on MODIS surface albedo data. *Geophys Res Lett* 32(21):L21410
- Notaro M, Liu ZY (2008) Statistical and dynamical assessment of vegetation feedbacks on climate over the boreal forest. *Clim Dyn* 31(6):691–712
- Notaro M, Vavrus S, Liu ZY (2007) Global vegetation and climate change due to future increases in CO₂ as projected by a fully coupled model with dynamic vegetation. *J Climate* 20(1):70–90
- Ogi M, Wallace JM (2007) Summer minimum Arctic sea ice extent and the associated summer atmospheric circulation. *Geophys Res Lett* 34(12):L12705
- O'ishi R, Abe-Ouchi A (2009) Influence of dynamic vegetation on climate change arising from increasing CO₂. *Clim Dyn* 33(5):645–663
- Oleson KW, Dai Y, Bonan G, Bosilovich M, Dirmeyer PA, Hoffman F, Houser P, Levis S, Niu GY, Thornton P, Vertenstein M, Yang Z-L, Zeng XB (2004) Technical description of the community land model (CLM). National Center for Atmospheric Research, Boulder, Colorado
- Overland JE, Wang M (2010) Large-scale atmospheric circulation changes are associated with the recent loss of Arctic sea ice. *Tellus A* 62(1):1–9
- Rayner NA, Parker DE, Horton EB, Folland CK, Alexander LV, Rowell DP, Kent EC, Kaplan A (2003) Global analyses of sea surface temperature, sea ice, and night marine air temperature since the late nineteenth century. *J Geophys Res-Atmos* 108(D14):4407
- Rothrock DA, Yu Y, Maykut GA (1999) Thinning of the Arctic sea-ice cover. *Geophys Res Lett* 26(23):3469–3472
- Schneider EK, Kirtman BP, Lindzen RS (1999) Tropospheric water vapor and climate sensitivity. *J Atmos Sci* 56(11):1649–1658
- Schuur EAG, Bockheim J, Canadell JG, Euskirchen E, Field CB, Goryachkin SV, Hagemann S, Kuhry P, Lafleur PM, Lee H, Mazhitova G, Nelson FE, Rinke A, Romanovsky VE, Shiklomanov N, Tarnocai C, Venevsky S, Vogel JG, Zimov SA (2008) Vulnerability of permafrost carbon to climate change: implications for the global carbon cycle. *Bioscience* 58(8):701–714
- Screen JA, Simmonds I (2010) The central role of diminishing sea ice in recent Arctic temperature amplification. *Nature* 464(7293):1334–1337
- Serreze MC, Walsh JE, Chapin FS, Osterkamp T, Dyurgerov M, Romanovsky V, Oechel WC, Morison J, Zhang T, Barry RG (2000) Observational evidence of recent change in the northern high-latitude environment. *Clim Change* 46(1–2):159–207
- Sitch S, Smith B, Prentice IC, Arneth A, Bondeau A, Cramer W, Kaplan JO, Levis S, Lucht W, Sykes MT, Thonicke K, Venevsky S (2003) Evaluation of ecosystem dynamics, plant geography and terrestrial carbon cycling in the LPJ dynamic global vegetation model. *Glob Change Biol* 9(2):161–185
- Solomon S, Intergovernmental Panel on Climate Change, Intergovernmental Panel on Climate Change. Working Group I. (2007) *Climate change 2007 the physical science basis: contribution of Working Group I to the Fourth Assessment Report of the Intergovernmental Panel on Climate Change*. Cambridge University Press, Cambridge
- Sturm M, Racine C, Tape K (2001) Climate change—Increasing shrub abundance in the Arctic. *Nature* 411(6837):546–547
- Swann AL, Fung IY, Levis S, Bonan GB, Doney SC (2010) Changes in Arctic vegetation amplify high-latitude warming through the greenhouse effect. *PNAS* 107(4):1295–1300
- Tape K, Sturm M, Racine C (2006) The evidence for shrub expansion in Northern Alaska and the Pan-Arctic. *Glob Change Biol* 12(4):686–702
- Thompson DWJ, Wallace JM (1998) The Arctic Oscillation signature in the wintertime geopotential height and temperature fields. *Geophys Res Lett* 25(9):1297–1300
- Tjernström M, Graverson RG (2009) The vertical structure of the lower Arctic troposphere analysed from observations and the ERA-40 reanalysis. *Q J Roy Meteor Soc* 135(639):431–443
- Tucker CJ, Slayback DA, Pinzon JE, Los SO, Myneni RB, Taylor MG (2001) Higher northern latitude normalized difference vegetation index, growing season trends from 1982 to 1999. *Int J Biometeorol* 45(4):184–190
- Walker MD et al (2006) Plant community responses to experimental warming across the tundra biome. *Proc Natl Acad Sci* 103(5):1342–1346
- Watson RT (2000) *Land use, land-use change, and forestry: a special report of the IPCC*. Cambridge University Press, Cambridge
- Zhang J, Walsh JE (2006) Thermodynamic and hydrological impacts of increasing greenness in Northern high latitudes. *J Hydrometeorol* 7(5):1147–1163
- Zhou L, Tucker CJ, Kaufmann RK, Slayback D, Shabanov NV, Myneni RB (2001) Variations in northern vegetation activity inferred from satellite data of vegetation index during 1981 to 1999. *J Geophys Res* 106(D17):20069–20083
- Zimov SA, Schuur EAG, Chapin FS (2006) Permafrost and the global carbon budget. *Science* 312:1612–1613